

Theoretical insights into the structures and fundamental properties of pnictogen nitrides

Jingjing Wang(王晶晶), Panlong Kong(孔攀龙), Dingmei Zhang(张定梅), Defang Gao(高德芳), Zaifu Jiang(蒋再富), and Wei Dai(戴伟)

Citation: Chin. Phys. B, 2024, 33 (**9**): 096201. DOI: 10.1088/1674-1056/ad6a07
Journal homepage: http://cpb.iphy.ac.cn; http://iopscience.iop.org/cpb

What follows is a list of articles you may be interested in

Chair-like N_6^{6-} in AlN_3 with high-energy density

Shi-Tai Guo(郭世泰), Zhen-Zhen Xu(徐真真), Yan-Lei Geng(耿延雷), Qi Rui(芮琦), Dian-Chen Du(杜殿臣), Jian-Fu Li(李建福), and Xiao-Li Wang(王晓丽)
Chin. Phys. B, 2023, 32 (**12**): 126202. DOI: 10.1088/1674-1056/acfd1a

Electronic structure and phase transition engineering in NbS_2: Crucial role of van der Waals interactions

Wei Wang(王威), Wen Lei(雷文), Xiaojun Zheng(郑晓军), Huan Li(黎欢), Xin Tang(唐鑫), Xing Ming(明星)
Chin. Phys. B, 2020, 29 (**5**): 056201. DOI: 10.1088/1674-1056/ab8214

Electronic structure of YbB_6 dependent on onsite Coulomb interaction U and internal parameter of B atom

Hong-Bin Wang(王宏斌), Li Zhang(张莉), Jie Duan(段婕)
Chin. Phys. B, 2019, 28 (**11**): 116201. DOI: 10.1088/1674-1056/ab46a1

First-principles investigations on structural stability, mechanical, and thermodynamic properties of LaT_2Al_{20} (T=Ti, V, Cr, Nb, and Ta) intermetallic cage compounds

Shanyu Quan(权善玉), Xudong Zhang(张旭东), Cong Liu(刘聪), Wei Jiang(姜伟)
Chin. Phys. B, 2018, 27 (**12**): 126201. DOI: 10.1088/1674-1056/27/12/126201

Theoretical study on the structural, mechanical, electronic properties and QTAIM of CrB_4 as a hard material

Xiao-Hong Li(李小红), Hong-Ling Cui(崔红玲), Rui-Zhou Zhang(张瑞州)
Chin. Phys. B, 2017, 26 (**9**): 096201. DOI: 10.1088/1674-1056/26/9/096201

Theoretical insights into the structures and fundamental properties of pnictogen nitrides

Jingjing Wang(王晶晶), Panlong Kong(孔攀龙)[†], Dingmei Zhang(张定梅), Defang Gao(高德芳), Zaifu Jiang(蒋再富)[‡], and Wei Dai(戴伟)[§]

School of Mathematics and Physics, Jingchu University of Technology, Jingmen 448000, *China*

(Received 4 May 2024; revised manuscript received 20 July 2024; accepted manuscript online 1 August 2024)

Recent experimental advancements reported a chemical reaction between antimony and nitrogen under high temperature and high pressure, yielding crystalline antimony nitride (Sb_3N_5) with an orthorhombic structure. Motivated by this statement, we calculate the stability, elastic properties, electronic properties and energy density of the $Cmc2_1$ structure for pnictogen nitrides X_3N_5 (X = P, As, Sb, and Bi) using first-principles calculations combined with particle swarm optimization algorithms. Calculations of formation enthalpies, elastic constants and phonon spectra show that P_3N_5, As_3N_5 and Sb_3N_5 are thermodynamically, mechanically and kinetically stable at 35 GPa, whereas Bi_3N_5 is mechanically and kinetically stable but thermodynamically unstable. The computed electronic density of states shows strong covalent bonding between the N atoms and the phosphorus group atoms in the four compounds, confirmed by the calculated electronic localization function. We also calculate the energy densities for Sb_3N_5 and find it to be a potentially high-energy-density material.

Keywords: pnictogen nitrides, structural stability, electronic property, energy density

PACS: 62.20.–x, 63.20.dk, 71.20.–b, 31.15.E– **DOI:** 10.1088/1674-1056/ad6a07

1. Introduction

Nitrogen is the first element in group 15 of the periodic table, constituting about 78% of Earth's atmosphere. It holds the distinction of being the most abundant uncombined element accessible to human beings. This abundance has driven the exploration of its applications, particularly in the field of high energy density materials (HEDMs).[1–4] Nitrogen possesses abundant electron valence states ($2s^2 2p^3$), enabling the formation of three types of bonds between nitrogen atoms: N–N single bonds, N=N double bonds, and N≡N triple bonds. Significant energy differences exist among the N–N single bond (∼ 167 kJ/mol), N=N double bond (∼ 419 kJ/mol), and N≡N triple bond (∼ 954 kJ/mol). Polynitrogen bonded in the form of a single or double bond can store substantial energy and release this chemical bond energy in an oxygen-free environment, decomposing into non-polluting nitrogen. Thus, polynitrogen emerges as a novel, green, and environmentally friendly high energy density material,[5] with significant application prospects in various fields including national defense, aerospace, and new energy.

High pressure has been proven to be the most effective technique in research of polymeric nitrogen synthesis. Various polynitrogen structures including nonmetal nitrides[6–12] and metal nitrides[13–18] have been successfully obtained using high-pressure techniques, greatly inspiring research enthusiasm. Recent studies have revealed that introducing metal elements into pure nitrogen under high pressure can induce the formation of new polynitrogen compounds with various polymerized nitrogen forms.[19] Currently, a range of theoretically predicted binary nitrogen-rich compounds with diverse configurations have been experimentally verified, including tetraza diene (N_4), pentazole (N_5), hexazine (N_6) and extended chains (N_∞). Nevertheless, research of binary crystalline nitrides involving group-15 elements significantly lags behind that of other nitrides, and these compounds continue to be an elusive class. Phosphorus elements (P, As, Sb, and Bi) possess an identical count of valence electrons as nitrogen, yet exhibit a greater atomic radius. This property facilitates the augmentation of chemical precompression within pnictogen nitrides while maintaining the compound's charge integrity. Consequently, one anticipates that pnictogen nitrides may serve as reservoirs for materials with elevated energy density, thereby offering a pathway towards the theoretical exploration of even more promising high energy density materials.

Recent progress in experimental investigations triggered a chemical reaction between antimony (Sb) and nitrogen (N_2) under elevated conditions of both high temperature (1600–2200 K) and high pressure (32–35 GPa). These extreme conditions were generated by employing a diamond anvil cell heated with a laser.[20] The resulting product of the reaction underwent identification through single crystal synchrotron x-ray diffraction at room temperature and 35 GPa. The analysis

[†]Corresponding author. E-mail: panlkong@163.com
[‡]Corresponding author. E-mail: 13986995705@163.com
[§]Corresponding author. E-mail: daiweiphysics@163.com

© 2024 Chinese Physical Society and IOP Publishing Ltd

revealed its composition as crystalline antimony nitride, conforming to the stoichiometry of Sb_3N_5, and possessing a structure categorized within the orthorhombic space group $Cmc2_1$. Motivated by the above statement, in this work we systematically investigate the structural stability, mechanical properties, electronic properties, chemical bonding and energy density for $Cmc2_1$ phase of pnictogen nitrides X_3N_5 (X = P, As, Sb, and Bi) by using the first-principles calculations. The findings of this study have significant practical implications across various fields such as material science, energy storage, aerospace, and defense. The high stability and energy density of pnictogen nitrides make them promising candidates for future applications that demand high-performance materials under extreme conditions. By providing a theoretical framework, this study paves the way for experimentalists to explore and develop these materials further.

2. Computation details

While experimental results propose that Sb_3N_5 adopts the $Cmc2_1$ phase, it remains vital and enlightening to systematically engage in computational studies for verifying and validating the structural distribution and associated atomic details. In pursuit of this objective, we employed the CALYPSO method for crystal structure search,[21–26] coupled with first-principles calculations, to execute predictions for the high-pressure structure of pnictogen nitrides (P_3N_5, As_3N_5, Sb_3N_5, and Bi_3N_5). Given only the chemical composition and pressure, without any experimental data, CALYPSO can successfully predict the most stable experimental structure.[27–30] The effectiveness of the CALYPSO method has been validated by testing nearly a hundred of known experimental structures.[31–36] We performed the evolutionary variable-cell structure predictions of pnictogen nitrides X_3N_5 (X = P, As, Sb, and Bi) containing up to 4 formula units (f.u.) at 0 GPa, 20 GPa, 40 GPa, 60 GPa, 80 GPa, and 100 GPa. The theoretical simulations of pnictogen nitrides involve the use of projector augmented wave (PAW) method[37] and electronic exchange correlations are managed using the Perdew–Burke–Ernzerhof (PBE) functional,[38] implemented in the Vienna *ab initio* simulation package (VASP).[39] Valence states for N, P, As, Sb, and Bi are $2s^22p^3$, $3s^23p^3$, $4s^24p^3$, $5s^25p^3$, and $6s^26p^3$, respectively. To ensure well-converged total energy calculations better than 1 meV per atom, a plane-wave kinetic energy cutoff of 800 eV and dense k-point grids with $5 \times 15 \times 15$ are selected. The phonon dispersion relations are calculated by using the PHONOPY code with the finite-displacement approach.[40]

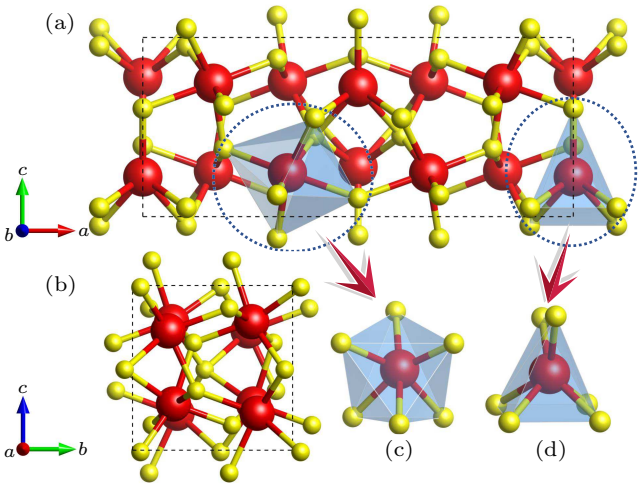


Fig. 1. [(a), (b)] Crystal structures and [(c), (d)] polyhedron views of $Cmc2_1$ phase for pnictogen nitrides along different crystallographic directions. The red and yellow spheres represent X and N atoms, respectively.

3. Results and discussion

The atomic arrangement depicting the $Cmc2_1$ phase of pnictogen nitrides X_3N_5 (X = P, As, Sb, and Bi) is illustrated in Fig. 1(a)1(b). This phase encompasses four X_3N_5 formula units per cell. Within the $Cmc2_1$ phase, two X atoms are situated at Wyckoff positions 8b (X01) and 4a (X02), and three N atoms are located at three Wyckoff sites 4a (N01), 8b (N02) and 8b (N03), respectively. Each X atom is coordinated by six neighboring N atoms, forming two distinct types of XN_6 units. Specifically, the X01 atoms exhibit hexa-coordination in Fig. 1(c), adopting a distorted hexahedral configuration with X–N separations spanning from 1.692 Å to 1.995 Å, 1.832 Å to 2.121 Å, 2.002 Å to 2.187 Å, and 2.105 Å to 2.291 Å for P_3N_5, As_3N_5, Sb_3N_5, and Bi_3N_5, respectively. In contrast, the X02 atoms are hexa-coordinated in a trigonal prismatic arrangement in Fig. 1(d), with X–N separations ranging from 1.753 Å to 1.966 Å, 1.896 Å to 2.095 Å, 2.063 Å to 2.236 Å, 2.171 Å to 2.342 Å for P_3N_5, As_3N_5, Sb_3N_5, and Bi_3N_5, respectively. Table 1 presents the equilibrium lattice parameters of the $Cmc2_1$ phase alongside reported experimental data. A comparison with Table 1 reveals that the lattice parameter and equilibrium lattice volume of Sb_3N_5 are consistent with the reported data. Furthermore, the equilibrium lattice volume of X_3N_5 (X = P, As, Sb, and Bi) follows the order of $P_3N_5 < As_3N_5 < Sb_3N_5 < Bi_3N_5$, aligning with the order of atomic radius of pnictogen. The calculated negative values of formation enthalpies for P_3N_5, As_3N_5, and Sb_3N_5, as listed in Table 1, show that they are thermodynamically stable at 35 GPa. The formation enthalpy of Bi_3N_5 is positive, indicating that it is thermodynamically unstable. The reduced electronegativity difference between Bi and N compared to other polynitrogens results in less polar and weaker Bi–N bonds. This contributes to the thermodynamic instability of Bi_3N_5 at ambient pressure due to decreased bond strength and stability.

Table 1. Calculated lattice parameters (Å), atomic coordinates and formation enthalpy (eV) per atom of pnictogen nitrides.

Unit cell	Lattice parameters	Atomic coordinates (fractional)	ΔH
P_3N_5	$a = 11.22$, $b = 4.33$, $c = 4.50$	P01(8*b*) (0.664, 0.754, 0.284)	−5.58
		P02(4*a*) (0.500, 0.715, 0.728)	
		N01(4*a*) (0.500, 0.905, 0.373)	
		N02(8*b*) (0.600, 0.558, 0.986)	
		N03(8*b*) (0.698, 0.105, 0.143)	
As_3N_5	$a = 11.91$, $b = 4.67$, $c = 4.84$	As01(8*b*) (0.665, 0.753, 0.282)	−0.85
		As02(4*a*) (0.500, 0.717, 0.727)	
		N01(4*a*) (0.500, 0.900, 0.366)	
		N02(8*b*) (0.600, 0.555, 0.987)	
		N03(8*b*) (0.695, 0.112, 0.148)	
Sb_3N_5	$a = 12.32$, $b = 5.10$, $c = 5.23$	Sb01(8*b*) (0.664, 0.756, 0.280)	−3.13
		Sb02(4*a*) (0.500, 0.722, 0.724)	
		N01(4*a*) (0.500, 0.896, 0.361)	
		N02(8*b*) (0.601, 0.549, 0.989)	
		N03(8*b*) (0.688, 0.120, 0.152)	
Sb_3N_5 [20]	$a = 12.31$, $b = 5.05$, $c = 5.19$	Sb01(8*b*) (0.664, 0.755, 0.277)	–
		Sb02(4*a*) (0.500, 0.723, 0.723)	
		N01(4*a*) (0.500, 0.896, 0.365)	
		N02(8*b*) (0.600, 0.550, -0.009)	
		N03(8*b*) (0.693, 0.115, 0.151)	
Bi_3N_5	$a = 12.86$, $b = 5.38$, $c = 5.47$	Bi01(8*b*) (0.665, 0.760, 0.275)	2.73
		Bi02(4*a*) (0.500, 0.723, 0.726)	
		N01(4*a*) (0.500, 0.893, 0.357)	
		N02(8*b*) (0.602, 0.545, 0.989)	
		N03(8*b*) (0.684, 0.130, 0.158)	

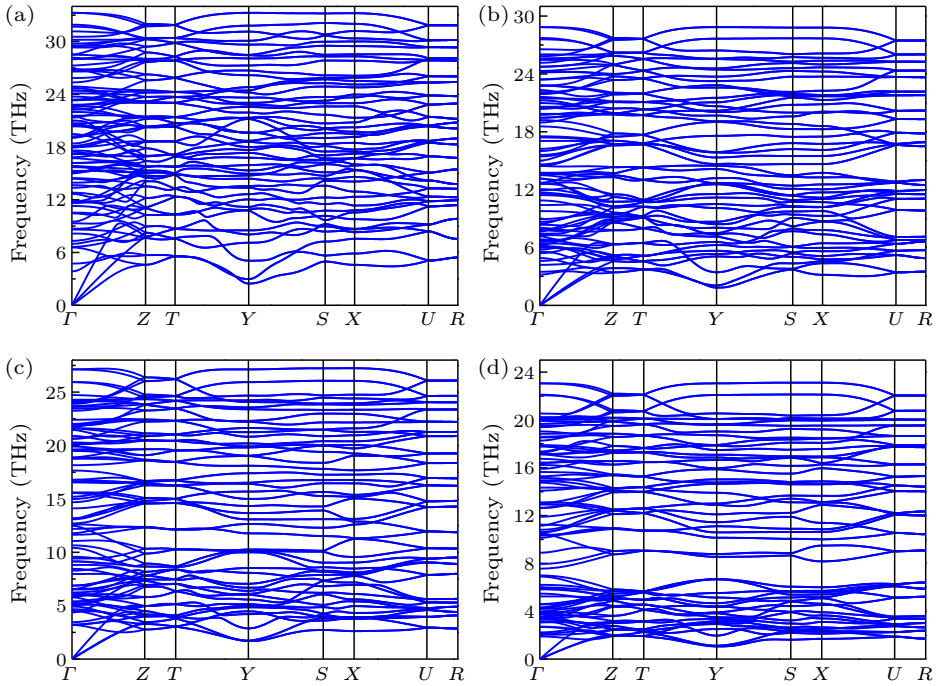


Fig. 2. Phonon dispersion curves of $Cmc2_1$ phase for pnictogen nitrides at 35 GPa: (a) P_3N_5, (b) As_3N_5, (c) Sb_3N_5, (d) Bi_3N_5.

In order to assess the mechanical and kinetic stability of X_3N_5 (X = P, As, Sb, and Bi), we have calculated their elastic constants using the stress–strain method and their phonon spectra using the finite displacement method,[41] respectively. The results are presented in Tables 2 and S1 (in the supporting information), Figs. 2 and S1 (in the supporting information). From the results of our calculated elastic constants, X_3N_5 (X = P, As, Sb, and Bi) all satisfy the mechanical stability criterion[42] at 35 GPa, indicating that they are mechanically stable. After pressure relief, at atmospheric pressure, Sb_3N_5 and Bi_3N_5 both satisfy the mechanical stability criterion and are mechanically stable. However, the elastic constants of both

P_3N_5 and As_3N_5 do not satisfy the mechanical stability criterion and are mechanically unstable at atmospheric pressure. The calculation of phonon spectra shows that X_3N_5 (X = P, As, Sb, and Bi) is kinetically stable with no imaginary frequencies appearing in the phonon spectra at 35 GPa, as well as Sb_3N_5 and Bi_3N_5 after the pressure relief. However, the imaginary frequencies appear in the phonon spectra of P_3N_5 and As_3N_5 after the pressure relief, which indicate that they are kinetically unstable.

Table 2. Calculated Constants C_{ij} (GPa), bulk modulus B (GPa), shear modulus G (GPa), B/G value, Young's modulus E (GPa), and Poisson's ratio ν of X_3N_5 (X = P, As, Sb, and Bi) at 35 GPa, respectively.

	P_3N_5	As_3N_5	Sb_3N_5	Bi_3N_5
C_{11}	574.99	421.15	373.91	290.79
C_{22}	928.94	616.54	529.11	358.29
C_{33}	1004.90	687.25	570.06	361.87
C_{44}	302.86	194.71	167.56	87.93
C_{55}	80.47	131.16	159.36	97.59
C_{66}	245.31	184.13	155.67	100.98
C_{12}	232.94	222.95	229.26	196.40
C_{13}	222.02	199.87	214.61	176.75
C_{23}	154.76	179.64	205.91	181.38
B	405.88	320.20	303.46	234.26
G	219.19	171.71	147.91	86.23
B/G	1.85	1.865	2.05	2.72
E	557.27	437.01	381.71	230.42
ν	0.271	0.273	0.290	0.336

In order to further investigate the elastic properties of X_3N_5 (X = P, As, Sb, and Bi), we calculated their bulk modulus B, shear modulus G, B/G value, Young's modulus E and Poisson's ratio ν using the VRH approximation method,[43] as listed in Table 2 for the results of the calculations. Generally speaking, the bulk elastic modulus characterizes the ability of the material to resist the volume change of the applied load, shear modulus characterizes the ability of the material to prevent the deformation in different directions caused by the applied load, Young's modulus is a physical quantity that characterizes the ability of the longitudinal resistance to the applied load, and Poisson's ratio ν is a physical quantity that expresses the ability of the longitudinal resistance to the applied load.[44,45] From Table 2, we can see that the magnitudes of B, G and E of X_3N_5 (X = P, As, Sb, and Bi) are in the order of $P_3N_5 > As_3N_5 > Sb_3N_5 > Bi_3N_5$, contrary to the magnitude of atomic radii of the nitrogen group elements. In addition, our results are significantly higher compared to previously reported theoretical data for Ta_3N_5 under high pressure.[46] It is noteworthy that the values of Young's modulus E are all larger than the bulk modulus B values for X_3N_5 (X = P, As, Sb, and Bi), which suggests that they are more resistant to tension than compression at 35 GPa. In contrast, the calculated Poisson's ratio ν of X_3N_5 (X = P, As, Sb, and Bi) is in the order of $P_3N_5 < As_3N_5 < Sb_3N_5 < Bi_3N_5$, which is the same as that of the atomic radii of the nitrogen group elements. Bi_3N_5 possesses the largest Poisson's ratio among the considered pnictogen nitrides, suggesting that it exhibits a more pronounced transverse expansion upon stretching. In order to evaluate the ductility of these structures, we also calculated their B/G values, and the results show that the B/G ratios of X_3N_5 (X = P, As, Sb, and Bi) are all greater than 1.75, indicating that they all have good ductile.[47]

To further understand the electronic properties of pnictogen nitrides, we calculated their band structures and density of states, as plotted in Fig. 3. The calculation of band structures shows that P_3N_5, As_3N_5 and Sb_3N_5 are semiconductors, where As_3N_5 and Sb_3N_5 belong to direct bandgap semiconductors with bandgaps of 0.57 eV and 0.60 eV, respectively. P_3N_5 belongs to indirect bandgap semiconductors possessing a bandgap of 1.94 eV. Interestingly, both valence and conduction bands in the band structure diagram of Bi_3N_5 appear to overlap, suggesting that it is metallic, as evidenced by the calculations of the density of states. From the density-of-states diagrams in Fig. 3, we can also see that the density-of-states compositions of these four compounds are very similar to the valence bands of their density of states that are mainly from the p state of the N atom, while the s states of the N atom and the X atom have very small contributions. It is worth noting that in these four compounds, there is a strong hybridization between the p state of N atom and the p state of X atom, which indicates that there are strong covalent bonds between these two atoms. In order to explore the bonding characteristics of pnictogen nitrides compounds in depth, we also calculated their electronic localization function (ELF), which can help us to distinguish metal, covalent and ionic bonds effectively. From Fig. 4, we can see that there is a strong electronic localization phenomenon for X–N in X_3N_5, indicating that there are strong covalent bonds between X and N. In addition, we have calculated the charges of each atom and Bader charges for pnictogen nitrides and summarized the calculations in Tables S2 and S3 (in the supporting information). From Tables S2 and S3, we can conclude that each N atom in P_3N_5, As_3N_5, Sb_3N_5 and Bi_3N_5 receives 1.88e, 1.30e, 1.43e and 1.23e charges from X atoms (X = P, As, Sb, and Bi), respectively. The charge transfer variations among the compounds of elements from the same group are quite significant. The reason is that the increase in atomic radius down the group results in longer bond lengths with nitrogen, leading to weaker orbital overlap and variations in charge transfer. Additionally, variations in electronegativity among the elements cause differences in their ability to attract electrons, leading to significant charge transfer differences. The calculation results of the Bader charges further confirm the existence of strong covalent bonding between X atoms (X = P, As, Sb, and Bi) and N atoms.

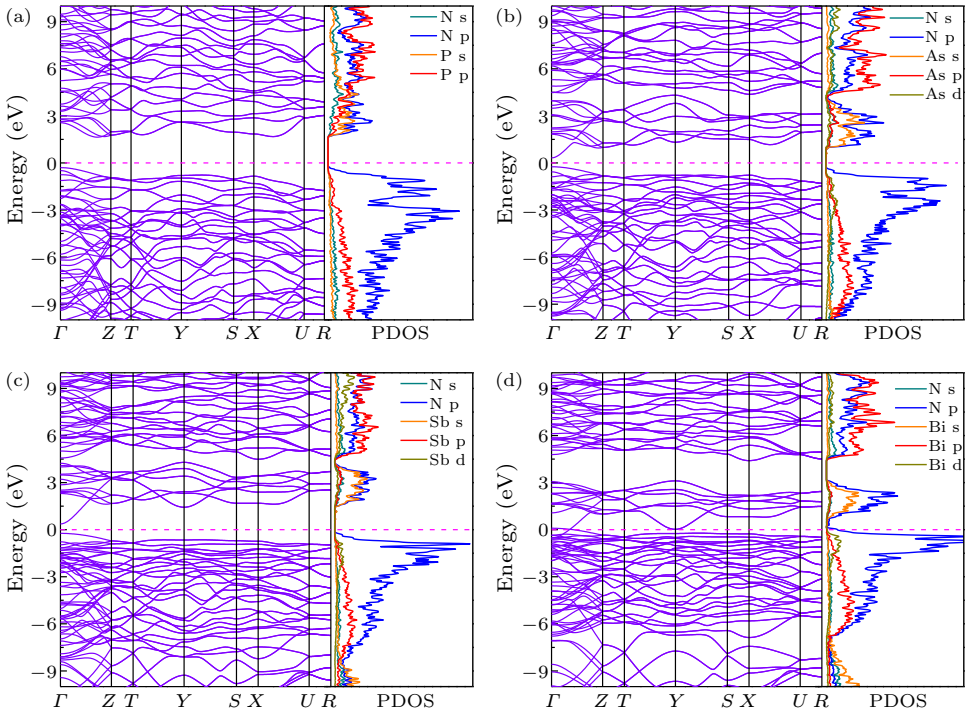


Fig. 3. Electronic band structure and DOS of $Cmc2_1$ phase for pnictogen nitrides at 35 GPa: (a) P_3N_5, (b) As_3N_5, (c) Sb_3N_5, (d) Bi_3N_5.

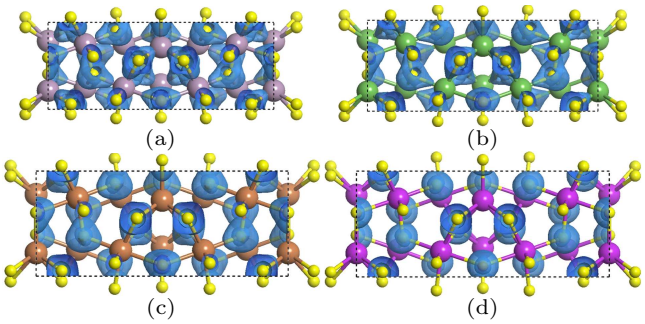


Fig. 4. Electron localization functions (ELFs) with an isosurface 0.75 of $Cmc2_1$ phase for pnictogen nitrides at 35 GPa: (a) P_3N_5, (b) As_3N_5, (c) Sb_3N_5, (d) Bi_3N_5.

Based on the above discussion, Sb_3N_5 is thermodynamically, mechanically and kinetically stable at both 35 GPa and atmospheric pressure after pressure relief. It also has strong covalent interactions in its structures to enhance its structural stability. In addition, Sb_3N_5 is expected to exothermically decompose into N_2 and solid Sb or Bi, and the chemical energy released from them during the reaction is 6.07 eV, respectively, which corresponds to energy densities of 1.35 $kJ{\cdot}g^{-1}$ in that order. Since its energy density is comparable to that of modern high explosives (1–3 $kJ{\cdot}g^{-1}$), such as TATB, HMX and RDX,[48] we consider it as a high-energy-density material.

4. Conclusion

Based on first-principles calculations combined with particle swarm optimization algorithms, we have systematically studied the stability, elastic properties, electronic properties, and energy densities of the $Cmc2_1$ structure for pnictogen nitrides X_3N_5 (X = P, As, Sb, and Bi). Calculations of formation enthalpies, elastic constants and phonon spectra show that they are all thermodynamically, mechanically and kinetically stable at 35 GPa. We have obtained the bulk modulus B, shear modulus G, and Young's modulus E for X_3N_5 (X = P, As, Sb, and Bi) using the results of calculated elastic constants and found that their magnitudes are in the opposite order to the magnitudes of the atomic radii of the nitrogen group elements. Interestingly, the calculated band structures and density of states show that As_3N_5 and Sb_3N_5 both belong to direct bandgap semiconductors with bandgap values of 0.57 eV and 0.60 eV, respectively. P_3N_5 belongs to direct bandgap semiconductors with bandgap value of 1.94 eV, while Bi_3N_5 is a metal. In addition, we have also calculated the energy densities for Sb_3N_5 and found it to be potential high-energy-density material. We hope that our calculations can provide some theoretical guidance for future experimental studies on the applications of pnictogen nitrides.

Acknowledgments

This work was supported by the Young Talent Project of the Scientific Research Plan by the Hubei Provincial Department of Education (Grant No. Q20234301), the Guiding Project of the Scientific Research Plan by the Hubei Provincial Department of Education (Grant No. B2023222), the Natural Science Foundation of Hubei Province (Grant No. 2022CFB527), the Scientific Research Project of Jingchu University of Technology (Grant Nos. YY202401,

YY202409, YY202207, and YB202212), and the Open Research Projects of Jingchu University of Technology (Grant No. HX20240009).

References

[1] Miao M S, Sun Y H, Zurek E and Lin H Q 2020 *Nat. Rev. Chem.* **4** 508
[2] Ji C, Adeleke A A, Yang L X, Wan B, Gou H Y, Yao Y S, Li B, Meng Y, Smith J S, Prakapenka V B, Liu W J, Shen G Y, Mao W L and Mao H K 2020 *Sci. Adv.* **6** eaba9206
[3] Laniel D, Geneste G, Weck G, Mezouar M and Loubeyre P 2019 *Phys. Rev. Lett.* **122** 066001
[4] Zhang L J, Wang Y C, Lv J and Ma Y M 2017 *Nat. Rev. Mater.* **2** 17005
[5] Christe K O, Wilson W W, Sheehy J A and Boatz J A 1999 *Angew. Chem. Int. Ed.* **38** 2004
[6] Zhang J, Zeng Z, Lin H Q and Li Y L 2014 *Sci. Rep.* **4** 4358
[7] Zhang S T, Zhao Z Y, Liu L L and Yang G C 2017 *J. Power Sources* **365** 155
[8] Yu S Y, Huang B W, Zeng Q F, Oganov A R, Zhang L T and Frapper G 2017 *J. Phys. Chem. C* **121** 11037
[9] Wei S L, Li D, Liu Z, Wang W J, Tian F B, Bao K, Duan D F, Liu B B and Cui T 2017 *J. Phys. Chem. C* **121** 9766
[10] Holtgrewe N, Lobanov S S, Mahmood M F and Goncharov A F 2016 *J. Phys. Chem. C* **120** 28176
[11] Liu Z, Li D, Wei S L, Wang W J, Tian F B, Bao K, Duan D F, Yu H Y, Liu B B and Cui T 2017 *Inorg. Chem.* **56** 7494
[12] Lian L L, Liu Y, Li D and Wei S L 2020 *RSC Adv.* **10** 2448
[13] Li Y W, Hao J, Liu H Y, Lu S Y and Tse J S 2015 *Phys. Rev. Lett.* **115** 105502
[14] Yin K T, Wang Y C, Liu H Y, Peng F and Zhang L J 2015 *J. Mater. Chem. A* **3** 4188
[15] Xia K, Sun J, Pickard C J, Klug D D and Needs R J 2017 *Phys. Rev. B* **95** 144102
[16] Li D, Tian F B, Lv Y Z, Wei S L, Duan D F, Liu B B and Cui T 2017 *J. Phys. Chem. C* **121** 1515
[17] Steele B A and Oleynik I I 2017 *J. Phys. Chem. A* **121** 1808
[18] Batyrev I G 2017 *J. Phys. Chem. A* **121** 638
[19] Ceppatelli M, Scelta D, Serrano-Ruiz M, Dziubek K, Morana M, Svitlyk V, Garbarino G, Poreba T, Mezouar M, Peruzzini M and Bini R 2022 *Angew. Chem. Int. Ed.* **61** e202114191
[20] Ceppatelli M, Serrano-Ruiz M, Morana M, Dziubek K, Scelta D, Garbarino G, Poreba T, Mezouar M, Bini R and Peruzzini M 2024 *Angew. Chem. Int. Ed.* **63** e202319278
[21] Wang Y C, Lv J, Zhu L and Ma Y M 2010 *Phys. Rev. B* **82** 094116
[22] Wang Y C, Lv J, Zhu L and Ma Y M 2012 *Comput. Phys. Commun.* **183** 2063
[23] Shao X C, Lv J, Liu P, Shao S, Gao P Y, Liu H Y, Wang Y C and Ma Y M 2022 *J. Chem. Phys.* **156** 014105
[24] Duan Q, Shen J, Zhong X, Lu H and Lu C 2022 *Phys. Rev. B* **105** 214503
[25] Sun W, Chen B, Li X, Peng F, Hermann A and Lu C 2023 *Phys. Rev. B* **107** 214511
[26] Lu C, Cui C, Zuo J, Zhong H, He S, Dai W and Zhong X 2023 *Phys. Rev. B* **108** 205427
[27] Duan Q, Zhan L, Shen J, Zhong X and Lu C 2024 *Phys. Rev. B* **109** 054505
[28] Zuo J, Zhang L, Chen B, He K, Dai W, Ding K and Lu C 2024 *J. Phys.: Condens. Matter* **36** 015302
[29] Chen B, He K, Dai W, Gutsev G L and Lu C 2023 *J. Phys.: Condens. Matter* **35** 183002
[30] Tong Q, Lv J, Gao P and Wang Y 2019 *Chin. Phys. B* **28** 106105
[31] Jin Y Y, Zhang J Q, Ling S, Wang Y Q, Li S, Kuang F G, Wu Z Y and Zhang C Z 2022 *Chin. Phys. B* **31** 116104
[32] Wang Y Q, Zhang C Z, Zhang J Q, Li S, Ju M, Sun W G, Dou X L and Jin Y Y 2023 *Chin. Phys. B* **32** 097402
[33] Wang Y, Cui X, Liu J, Jing Q, Duan H and Cao H 2023 *Chin. Phys. B* **33** 016109
[34] Guo S T, Xu Z Z, Geng Y L, Rui Q, Du D C, Li J F and Wang X L 2023 *Chin. Phys. B* **32** 126202
[35] Liu P, Xu M, Lv J, Gao P, Huang C, Li Y, Wang J, Wang Y and Zhou M 2022 *Chin. Phys. B* **31** 106104
[36] Pu C Y, Yu R M, Wang T, Xüe Z Y, Zhu Y S and Zhou D W 2021 *Chin. Phys. B* **30** 017102
[37] Blöchl P E 1994 *Phys. Rev. B* **50** 17953
[38] Perdew J P, Burke K and Ernzerhof M 1996 *Phys. Rev. Lett.* **77** 3865
[39] Kresse G and Furthmüller J 1996 *Phys. Rev. B* **54** 11169
[40] Togo A, Oba F and Tanaka I 2008 *Phys. Rev. B* **78** 134106
[41] Yin M T, and Cohen M L 1982 *Phys. Rev. B* **26** 3259
[42] Wu Z J, Zhao E J, Xiang H P, Hao X F, Liu X J and Meng J 2007 *Phys. Rev. B* **76** 054115
[43] Hill R 1952 *Proc. Phys. Soc. London A* **65** 349
[44] Zhang J, Wang Y, Tang L, Duan J, Wang J, Li S, Ju M, Sun W, Jin Y and Zhang C 2022 *Arabian J. Chem.* **15** 104347
[45] Haines J, Léger J and Bocquillon G 2001 *Annu. Rev. Mater. Res.* **31** 1
[46] Li D, Tian F, Duan D, Bao K, Chu B, Sha X, Liu B and Cui T 2014 *RSC Adv.* **4** 10133
[47] Wang J J, Hermann A, Kuang X Y, Jin Y Y, Lu C, Zhang C Z, Ju M, Si M T and Iitaka T 2015 *RSC Adv.* **5** 53497
[48] Evans W J, Lipp M J, Yoo C S, Cynn H, Herberg J L, Maxwell R S and Nicol M F 2006 *Chem. Mater.* **18** 2520